Hindawi
Complexity
Volume 2022, Article ID 8539326, 16 pages
https://doi.org/10.1155/2022/8539326

Research Article

UAVs Protection and Countermeasures in a Complex Electromagnetic Environment

Anton O. Belousov, Yevgeniy S. Zhechev, Evgeniya B. Chernikova, Alexander V. Nosov, and Talgat R. Gazizov

Department of Television and Control, Tomsk State University of Control Systems and Radioelectronics, Tomsk, Russia

Correspondence should be addressed to Anton O. Belousov; ant1lafleur@gmail.com

Received 3 March 2022; Revised 30 April 2022; Accepted 17 June 2022; Published 13 July 2022

Academic Editor: Chao Liu

The study considers the problem of ensuring electromagnetic compatibility of EMI-based functional destruction means with other radioelectronic equipment as part of a complex for countering unmanned aerial vehicles. To solve this problem, it is proposed to create a methodology that combines a set of diverse approaches and methods. This study focuses on the use of hollow and thin passive conductors, the use of a magnetodielectric in a reflection symmetric modal filter, the use of reflection symmetric structures for decomposing the train of ultrashort pulses (USP), and the use of a meander line as a protective means against USPs. The main results that are expected to be obtained using the proposed approaches and methods are outlined.

1. Introduction

The last decade has been marked by intensification in the development of unmanned aerial vehicles (UAVs) because of their proliferation not only in the civilian but also in the military areas. UAVs make it possible to significantly reduce the cost of services related to remote and real-time monitoring of the environment and objects, compared with traditional space or aviation systems [1–3]. Meanwhile, this time also witnesses the appearance of improved medium and small UAVs, which makes the tasks of countering them in highly controlled areas particularly urgent [4, 5]. In addition, modern UAVs are used as one of the most important means of increasing the combat capabilities of the armed forces. Since UAVs have become widespread in military domain, intense research and development activities in this area has started, as can be seen from the works [6–10]. At the same time, this issue is relatively new, since the earliest work on the topic of countermeasures against UAVs [8] dates back to 2008, and the beginning of active scientific publications on this topic dates back to 2016–2017.

It is well-known that the task of countering UAVs (which arose in the early 2000) can be solved in various ways: from the use of fire weapons (i.e., air defense) and electronic countermeasures against critical UAV systems to direct physical interception of UAVs and the use of EMI-based functional destruction means. The latter method seems to be the most promising, since it is devoid of the most serious drawback of electronic countermeasures means–the lack of an unambiguous reaction of the UAV to successful suppression. However, the EMI-based functional destruction means operate using the generators of powerful microwave and laser radiation. The examples of such EMI generators can be electromagnetic installations (electromagnetic accelerators or simply guns), explosive magnetic generators, warheads of antiaircraft guided missiles, and antiaircraft artillery shells with emitters of powerful electromagnetic microwave pulses. Consequently, the high power of the generated EMI and the difficulty of ensuring its selectivity in relation to the affected radioelectronic equipment (REE) worsen the internal electromagnetic environment inside the UAV countermeasures complex. In particular, the difficulty in ensuring the selectivity of the EMI excitation can lead to

malfunctions of the elements of «friendly» REE (receiving and transmitting devices, signal generators, control, stabilization, command generation devices, and various electronic computers). The reason for such malfunctions can be as follows: excesses in useful signal amplitudes caused by crosstalk, the overlapping of useful signal spectra with interference ones, the overlapping of interference pulses in device circuits on generated useful signals and their superposition in time, and crosstalk in external and internal circuits. It raises the issue of ensuring electromagnetic compatibility (EMC) of the EMI-based functional destruction means with other REE as part of the UAV countermeasures complex. Another important issue is ensuring the EMC of «friendly» UAVs, which may be in the damage area of the EMI-based functional destruction means.

The reason why this issue has not been raised before is probably because the price of small UAVs is not high (in contrast to the prices of military equipment or ammunition). However, the additional «survivability» of UAVs can be of great help during real combat operations. Another reason is that ensuring the EMC of UAV countermeasures systems can be expensive. However, recently obtained investigation results for the first time can be exploited to find the ways to solve this problem. In addition, it could be possible without resorting to large financial costs.

Much attention is paid to the problem of UAV protection and countermeasures in complex electromagnetic environment. It is evidenced by the scientific work presented in the next section. However, the methodological aspects have not been studied enough. Hence, the authors are not aware of scientific works or standards devoted to the description of a unified methodology for ensuring the EMC of the UAV countermeasures complex that employs EMI-based functional destruction means. The aim of this work is to fill this gap by presenting preliminary results on such a methodology. To achieve this, several approaches and methods are discussed to create this methodology. In addition, the results that confirm the efficiency and applicability of some of them are presented. Thus, the overall contribution of this study in developing such a scientific direction has been motivated by new effective approaches to creating the methodology for ensuring EMC. These approaches are designed to eliminate significant shortcomings in the effectiveness of EMI-based functional destruction means that were mentioned earlier.

The article is divided into several sections. There are numbered, taking into account the sequence order, starting with section 2. Section 2 presents a brief review of scientific studies on the subject of the study. Section 3 highlights the proposed approaches and methods. In Sections 4–8, the feasibility of the proposed methods and approaches is demonstrated. Section 4 is devoted to modal filtration. Section 5 describes the method of hollow and thin passive conductors. Section 6 is devoted to the use of magnetodielectric in structures with modal reservation. Section 7 assesses the evaluation of ultrashort pulses (USP) train attenuation possibility. Section 8 considers the use of a meander lines (ML) as a mean of USP protection. The results are discussed in section 9 and summarized in section 10.

2. Brief Review of Related Scientific Works

There is a well-known work [11] that investigates the ultrawideband (UWB) electromagnetic pulse (EMP) effects on commercial DJI Phantom 3 Standard UAV. It was found that the UAV is vulnerable to UWB EMPs. The authors obtained the parameters of emitted pulses and classified the types of equipment faults. They also proposed the characteristics of UWB EMP emitter prototype used for UAV jamming. Since investigations of the influence of electromagnetic environment on UAVs have become relevant in recent years, a novel method is presented to test the susceptibility of UAVs to intentional electromagnetic interference [12]. Using this method, UAVs are tested on susceptibility to radiated continuous waves. The results show that even if the radiated electric field is lower than 1 V/m, the data link that is used by a UAV to communicate with the ground control station can be disrupted. It happens when the frequency of the radiated continuous wave is the same as, or close to, the UAVs data link. Some of the sensitive frequencies, such as 1/2, 1/3, 1/4, and 1/5 times of the working frequency, could lead to the disruption of the data link because of the harmonics produced by nonlinear units. Another study [13] describes a high-power microwave weapon that has many advantages to fight against UAVs. The basic concept of high-power pulse interference is introduced, and the feasibility of the EMI against UAVs is discussed. A change in the UAV normal operation mode was demonstrated with the help of simulation software. The work [14] presents a new model of the UAV datalink in different flight states. The relationship between the airborne operation signal, the induced interference, and the flight parameters is presented and compared in three typical flight states, i.e., the fixed angle state, dive state, and hover state. The article [10] deals with the issue of eliminating UAVs using nondestructive methods with the emphasis on possible electronic warfare applications. The results of the work summarize possible anti-UAV defense means and evaluate their potential defense potential. The article [15] proposes a warning technique in case a possible EMI appears near the UAV, which is based on semantic analysis. The data source for semantic analysis is collected based on the subtle changes of the UAV state parameters during the EMI interference process. The article [16] evaluates the effectiveness of the use of high power directed energy weapons as a method to neutralize civilian UAVs. In [17], various propulsion systems currently used in UAVs are analyzed. In doing so, special attention is paid to the characteristics that are essential to conduct a specific mission, including geological and photogrammetric ones. The book [18] details the aspects of countering a huge range of civil and military UAVs and their respective system components. The article [19] analyzes the EMI characteristics of the converter station equipment in the surrounding area and the EMI impact on the UAV communication circuits. The anti-EMI countermeasures strive to eliminate or reduce the EMI threats on the UAV hardware and its communication network. In [20], the latest accidents with medium and heavy UAVs in the past 10 years are analyzed. Combined with the performance and technical

characteristics of each device, the accident stages, causes, and rules are classified, summarized, and analyzed in detail, and the accident trend is predicted. In [21], various studies on the effect of intentional EMI on UAVs are considered. They are reviewed and classified on the basis of the power level, preset information, and frequency. The article [22] presents the results of the experimental tests of the pulse response of a UAV and its essential components. A standardized lightning pulse that is often used during equipment immunity tests in the aviation industry was applied. A model was built on the basis of the transmittance of the circuits that are most exposed to lightning surges. The article [23] presents the development and examination of genetic algorithms to solve the multicriteria problems of placing the onboard equipment inside UAV fuselage. In addition, the criteria for the EMC of onboard equipment with external, intersystem, and intrasystem electromagnetic effects are considered.

Meanwhile, since information technologies, especially wireless communications, are rapidly developing, the problem of EMC between systems is becoming more important. The article [24] reviews the literature on the EMC subject that is devoted to EMI that may affect data links operating between UAVs and ground stations. The study [25] describes the possibilities of developing innovative experimental and numerical approaches to assess the EMC of UAVs under high EMI intensity, such as lightning and nonnuclear electromagnetic pulses. The article [26] considers the electromagnetic environment of UAV systems and analyzes the features of the EMI impact. The numerical modeling of various EMIs, their experimental testing, and proposals on EMC are considered. In [27], the researchers investigate the influence of intentional EMI on the sensors of a UAV, which is a small serial quadrocopter. The interfering signal is a narrowband high-power electromagnetic pulse characterized by frequencies between 100 MHz and 3.4 GHz and field strengths that are above the immunity levels required by EMC standards. In [28], the interference that occurs between the main UAV systems and the CDMA system is investigated using the Simulink software. The work [29] describes the measurements of potential interference spectra in a powerful electrical environment of a large UAV, which is viewed as a platform for installing equipment for measuring electromagnetic fields. The equipment includes an electromagnetically compatible transponder antenna for a tactical automatic landing system. The proposed repeater antenna has a monopole radiator designed for X-band operation in UAV guidance applications, and a protective metal cover to suppress unwanted RF interference. The mechanisms of electromagnetic coupling between the antenna and the neighboring conductive devices are also being studied to develop transponder antenna layout guidelines [30]. The measurements inside the UAV fuselage could also be carried out using a new loop probe with a double load, as described in [31].

The UAV EMC issues are presented in detail in two separate perspectives: radiation and noise immunity [32]. Small UAVs usually include satellite navigation, inertial navigation, and magnetic compass systems. Solid state inertial sensors are used to maintain the position of a UAV during flight, and a compass can be used to determine the correct azimuth orientation. To study the effect of a powerful microwave pulse on the UAV data transmission channel during dynamic flight, it is proposed to use the interference tracking model for a powerful microwave pulse source in the direction of the UAV [33]. In addition, a dynamic flight model is being built to determine the reception of a powerful UAV microwave pulse. To predict the possible impact of a powerful microwave pulse on a data channel, tests on a certain type of UAV data link are carried out in the presence of a powerful microwave pulse with its carrier frequency in the L-, S-, and C-bands, respectively. The results show that EMI can easily enter the receiver through the antenna when the carrier frequency of a high-power microwave pulse falls within the operating bandwidth of the data link, causing permanent physical damage. Finally, the importance of the task of countering UAVs (and especially small UAVs) is confirmed by a large number of relevant works on this topic, for example, those presented in the book [34].

3. Suggested Approaches and Methods

The creation of any methodology implies the development of theoretical foundations, methods, basic principles, process, and means of their implementation, aimed at solving specific problems. In this case, the problem is to provide the EMC of EMI-based functional destruction means with other REE as part of the UAV countermeasures complex. To solve this sophisticated problem, a novel set of diverse approaches and methods are presented. They are given in Table 1.

In the following sections, the feasibility of the proposed methods and approaches is demonstrated on some examples, which are as follows: modal filtration, which is a method of hollow and thin passive conductors on the example of a 2-conductor MF based on a conventional microstrip line (MSL), a magnetodielectric for a reflection symmetric MF with a triple MR as a resource for increasing the attenuation of the interference signal, a reflection symmetric MF and an ML as a result of TRIZ application when they are exposed to a train of USPs, and an ML as a means of protection against USPs.

4. Modal Filtration

The level of the resulting voltage at the MF output is determined by various factors, namely the geometric configuration of the protective device, the number of conductors, the dielectric material used, and the length. Thus, a conventional MF based on a coupled transmission line is shown in Figure 1, where w is the width of the conductors, s is the distance between the conductors, t is the thickness of the conductors, h is the thickness of the dielectric, d is the distance from the edge of the structure to the conductors, and ε_r is the relative permittivity of the substrate (Figure 1(a)). The length (l) of the MF was taken equal to 1 m. As an excitation pulse, an EMF source with a USP in the form of a trapezoid was used with an amplitude of 1 V and the durations of the rise, fall, and flat top (at levels 0–1) of 100 ps, so that the total duration was 300 ps (Figure 1(b)).

Table 1: Suggested approaches and methods.

Title	Description
A priori awareness of «friendly» impact, possibly from a database (from open sources like [35]) of the characteristics of EMI-based functional destruction means	A priori knowledge of the specific parameters of the induced interference (for example, a dangerous USP) on numerous REE operating as a part of the UAV opens up the possibility of ensuring the operation of «friendly» UAVs after it being affected by EMI-based functional destruction means.
The use of the theory of inventive problem solving (TRIZ) as part of a diversionary approach [36]	TRIZ guarantees the discovery of hidden resources. The theoretical foundations of TRIZ are the laws of technical system development, formulated as a result of analyzing large arrays of patents, and studying the history and logic of technical system development. TRIZ is built as an exact science that has its own field of study, its own methods, its own language, and its own tools. In addition, TRIZ can be effectively used as part of a diversionary approach to identify weaknesses in case of deliberate impacts.
Modal filtration [37]	This method involves the protection of critical circuits of REE by means of the sequential decomposition of ultrashort pulses (USPs) into a sequence of pulses (because of the difference between mode delays in the transmission line) with much lower amplitudes. Devices based on this technique are called modal filters (MF).
The use of the method of hollow and thin passive conductors in an MF [38]	The method of hollow and thin passive conductors proposed in the Russian Foundation for Basic Research project for spacecraft reduces the mass of MF. In particular, UAV supporting structures can be employed. Placing transmission lines along them can form a protective structure.
Modal reservation (MR) of circuits [39, 40]	Complex reservation of UAV circuits at the level of components, boards, and cables ensures the survivability of the UAV using modal decomposition. A number of studies have been carried out directly on the hybridization of reservation and modal filtration into a single whole. They prove the possibility to successfully and efficiently apply MR. In this case, multicriteria optimization will be used to improve protection and reduce the mass of conductors and dielectrics.
Considering the possibility of dangerous USP impact bypassing protective means [41]	USP protection at a junction of the segments in coupled lines that have the opposite signs of the differences in per-unit-length delays of even and odd modes may be useless. The reason for this may be the USP decomposition into smaller amplitude pulses at this junction with its further recovery at the end of the structure.
The use of a spiral power bus [42]	A spiral power bus proposed for a spacecraft within the framework of the RFBR grant, which is used to protect the UAV, adds a minimum increase in the mass. This approach could reduce the mass and inductance of the bus at the same current load, utilize a minimum number of connectors, and shield (inside this bus) other conductors that are connected to critical nodes.
The use of a protective ML [43]	An ML in air dielectric filling (or an air ML) differs by a complete lack of a dielectric and a single frequency response in a wide frequency band. Nevertheless, it can decompose the USP of unlimited voltage into 2 main pulses of lower voltages. Microstrip MLs allow for USP decomposition into 3 or even 4 pulses.
Resonance shift in the body slots caused by their overlap with a thin magnetodielectric [44, 45]	New models that could set the values of the relative dielectric and magnetic permeability can be selected in accordance with the spectrum of the destructive impact for the masking or protective shift of resonances in the body slots because of their overlap with a thin magnetodielectric.
The use of software tools adapted for the goals of the work [46]	Software tools provide a complex estimation of how efficient the protection against arbitrary influences is according to the criterion of reducing 5 standard N-norms of the time response. They also enable optimization with any set of criteria using a genetic algorithm.

The resistance values (R) were chosen from the condition of matching the structure with the path (the signal amplitude at the beginning of the line (V_2) should be equal to half the EMF of the signal source (V_1) (Figure 1(c)) [47].

5. Method of Hollow and Thin Passive Conductors

UAVs performance could be improved by embedding REE elements or protective devices. At the same time, the minimum increase in mass is very important when developing new UAV designs or improving the existing ones. In this regard, it is effective to employ protective MFs that involve hollow and thin passive conductors. This approach reduces the mass of the final product while maintaining the protective characteristics. For clarity, it is demonstrated on MF prototypes with increased geometric dimensions (relative to the designs used in real UAVs). What follows demonstrates the main results on the design and building these prototypes. The main structures with hollow and thin passive conductors and their geometric and circuit models are shown. A full-scale experiment on measuring the characteristics of the MF is described. The calculated and measured characteristics of the MF are compared.

The cross-sections and the equivalent circuit of the prototypes are shown in Figure 2. The cross-sections have the following parameters: $w = 10$ mm, $s = 0.5$ mm, $t = 10$ mm (in case of the MF with a thin passive conductor $t = 1$ mm), $h = 1.5$ mm, $g = 1$ mm (wall thickness of conductors), $\varepsilon_r = 4.6$, and $tg\delta = 0.025$ (dielectric loss tangent). The parameters of the circuit are as follows: $R_G = R_L = 50\,\Omega$, and $R = 10\,\Omega$ for the MF with solid, hollow, and corner passive conductors; and $R = 13\,\Omega$ for the MF with a thin passive conductor to approximate the values of the mean geometric

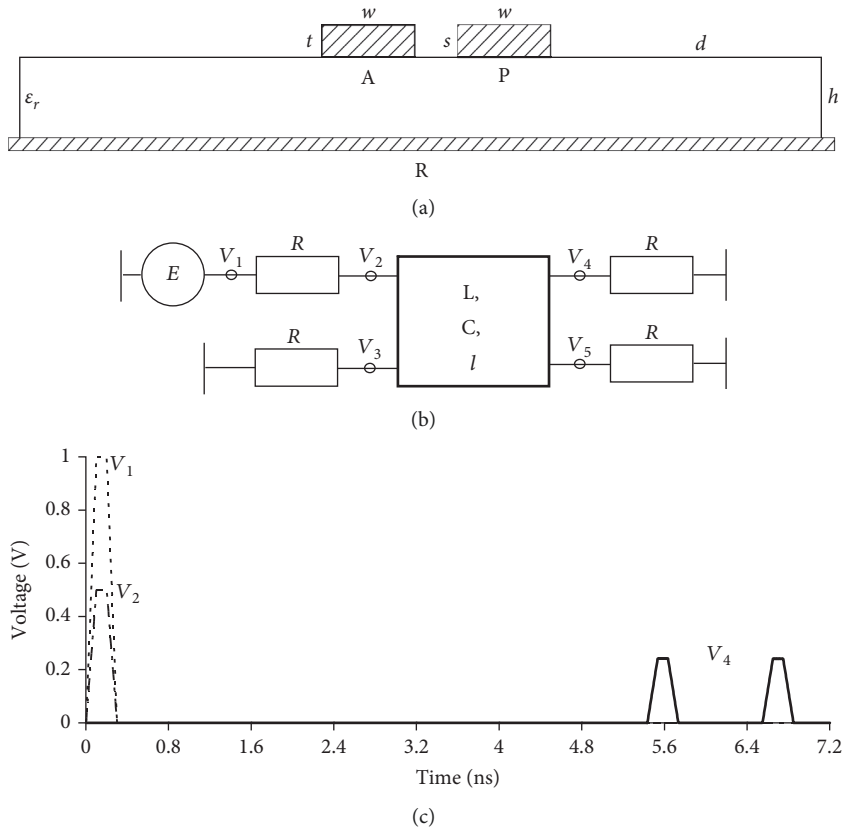

Figure 1: (a) Cross-section of the MF based on the coupled line, (b) its equivalent circuit, and (c) waveforms (V_1) of the EMF and voltages (V_2) at the input and (V_4) output of such an MF.

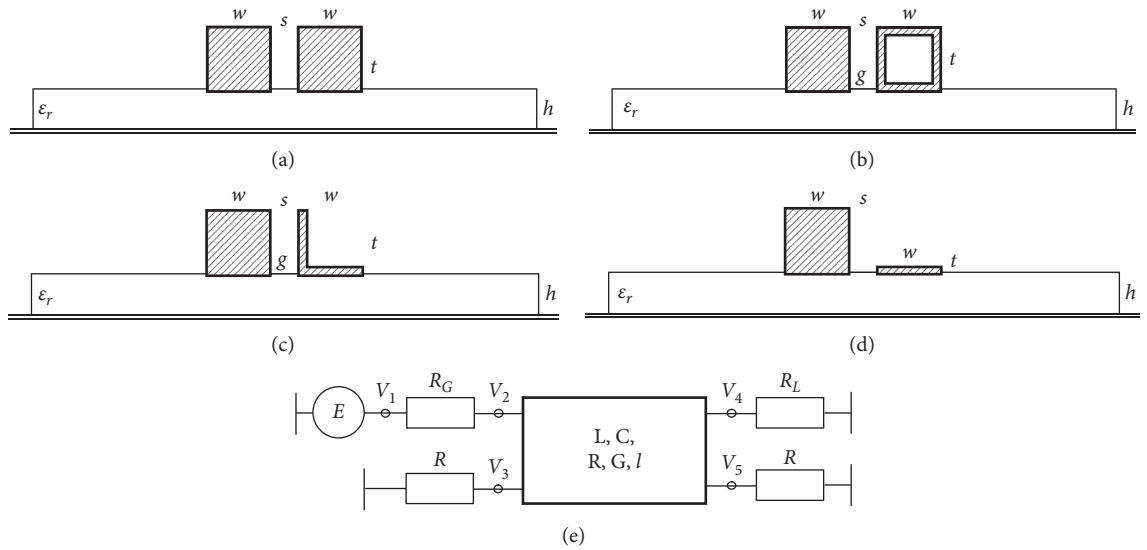

Figure 2: Cross-sections of the MF with passive conductors: (a) solid, (b) hollow, (c) corner, (d) thin, and their (e) equivalent circuit.

resistances of the even and odd MF modes. The lengths (l) of all MFs are 28 cm.

A full-scale experiment was conducted using the approach from [48]. In this case, the time and frequency characteristics were calculated in the ADS system based on the experimentally obtained S-parameters. After the MFs under study were measured in the frequency domain, they were analyzed in the time domain in the ADS 2020 system. The device defined in the frequency domain was represented as an n-port device. It is described by equations that show the relation between the spectral variables of each port. Since the parameters of the scattering matrix (output format of the

S2P type) were determined for the MFs that are coupled MSLs, their circuit in ADS 2020 appeared to be a 2-port device.

The method of determining the time and frequency characteristics based on the measured *S*-parameters was used to describe the signal propagation through the MF so it is possible to use any form of influence. Therefore, an ideal trapezoidal pulse signal was used with an EMF amplitude of 1 V and the duration of the rise, fall, and flat top of 100 ps each (total duration was 200 ps at a level of 0.5).

The prototypes of the MFs are shown in Figure 3. To make the measurements more convenient, a single FR-4 dielectric substrate (obtained from a compound of 2 FR-4 substrates) was used. In this case, one of the conductors (active) is fixed, and the second is removable. Thus, the passive conductor in the MF can be replaced to measure the characteristics under the same conditions. To ensure the fixation and integrity of the structure, as well as the specified separation between the conductors, recesses were made in the substrate to accommodate the conductors. The recesses were 10 mm wide and 300 μm high. After fixing the conductors into the recesses, they were soldered along the edges for additional fixation and electrical contact (the active conductor was additionally placed on a thin layer of epoxy glue). SMA-connectors were installed at the ends of the active (solid) conductor.

The results of a full-scale experiment on measuring the MF characteristics with solid, hollow, corner, and thin passive conductors are considered in the time and frequency domains. The measuring setup with the MF prototype with a corner passive conductor is shown in Figure 4 (the rest of the passive conductors lie on the table). Figure 5 shows the frequency dependences of $|S_{21}|$ for each MF (measured by the vector network analyzer «Panorama» P4226).

It follows from the measurement results that the bandwidth of all MFs is 77–82 MHz. The frequency dependences of $|S_{21}|$ for the MF with solid, hollow, and corner passive conductors are very close. In this case, the frequency dependence of the MF with a thin passive conductor has significant differences from as high as 2.5 GHz.

$U(t)$ dependences at the output of all MFs, obtained by the experiment and the simulation that took into account losses, are shown in Figure 6. The values of the maximum output voltage for solid, hollow, corner, and thin passive conductors were 0.177, 0.178, 0.192, and 0.251 V during the measurements and 0.116, 0.117, 0.119, and 0.151 V during the simulation, respectively. The maximum deviation of the obtained values during the measurements and simulation was ±25% for the MF with a thin passive conductor. The measurements showed that the values of the maximum output voltage are 5.6, 5.61, 5.2, and 4 times less than the EMF amplitude.

It can be seen that the output signal arrives at approximately the same time with an average deviation of ±3% for the odd (early) mode. Unfortunately, because of the dispersion, it is impossible to accurately determine the arrival time of each pulse during measurements. In addition to dispersion, the voltage waveforms are affected by losses in conductors and dielectrics. It leads to an increase in the rise and fall times of each output pulse and to their partial superposition, which is clearly observed for the MF with a thin passive conductor. In addition, the pulse amplitudes obtained by the simulation and experimentally differ (despite the fact that in both cases, the active conductor was loaded by 50 Ω and the passive conductor by 10 Ω for the MF with solid, hollow, and corner passive conductors, and 13 Ω for the MF with a thin passive conductor). The reason probably lies in the reflections caused by the mode mismatch, which are clearly manifested during the measurement. Thus, the first sequence of reflections is observed in the range of 3.4–7 ns (not shown in Figure 6 because it was important to detail the main output signal). Additionally, reflections caused by inhomogeneities that arrived at the end of the MF are superimposed on the main mode pulses (mainly on the even pulse (pulse 2)), leading to an increase in the resulting amplitude. It also explains the difference between the pulse amplitudes when simulating and measuring the MF with a thin passive conductor. Despite this, the modal filtration effect is seen to be preserved when the passive conductor of the MF is replaced. In general, there is consistency in the output voltage waveforms obtained experimentally and by the simulation.

Next, the mass of the developed MFs was estimated. Since the filters differ only in the passive conductor, its mass was estimated for various MF configurations.

With $w = 10$ mm, $t = 10$ mm, $g = 1$ mm, $l = 30$ cm, and aluminum density $\rho = 2.71$ g/cm^3, the volume of a solid conductor is as follows:

$$V = lwt = 30\,\text{cm}^3, \tag{1}$$

and the mass is as follows:

$$m = V\rho = 81.3\,\text{g}. \tag{2}$$

The conductor cavity volume is as follows:

$$V_h = (l\text{–}2\text{g})\,(\text{w}\text{–}2\text{g})\,(\text{t}\text{–}2\text{g}) = 19.072\text{cm}^3, \tag{3}$$

and the mass of a hollow conductor is as follows:

$$m_h = (V\text{–}\text{V}_\text{h})\rho = 29.615\,\text{g}, \tag{4}$$

which is almost 3 times less than the mass of a solid conductor.

The corner conductor mass is as follows:

$$m_\text{C} = \frac{m_h}{2} = 14.807\,\text{g}, \tag{5}$$

which is 5.5 times less than the mass of a solid conductor.

For a thin conductor, according to (1) and (2) at $t = 1$ mm, the volume will be 3 cm^3, and the mass will be 8.13 g, which is 10 times less than the mass of a solid conductor.

6. Magnetodielectric in Structures with Modal Reservation

Redundancy is used to increase the reliability of REE. Engineers widely use cold redundancy because of the low complexity of its implementation. This approach provides

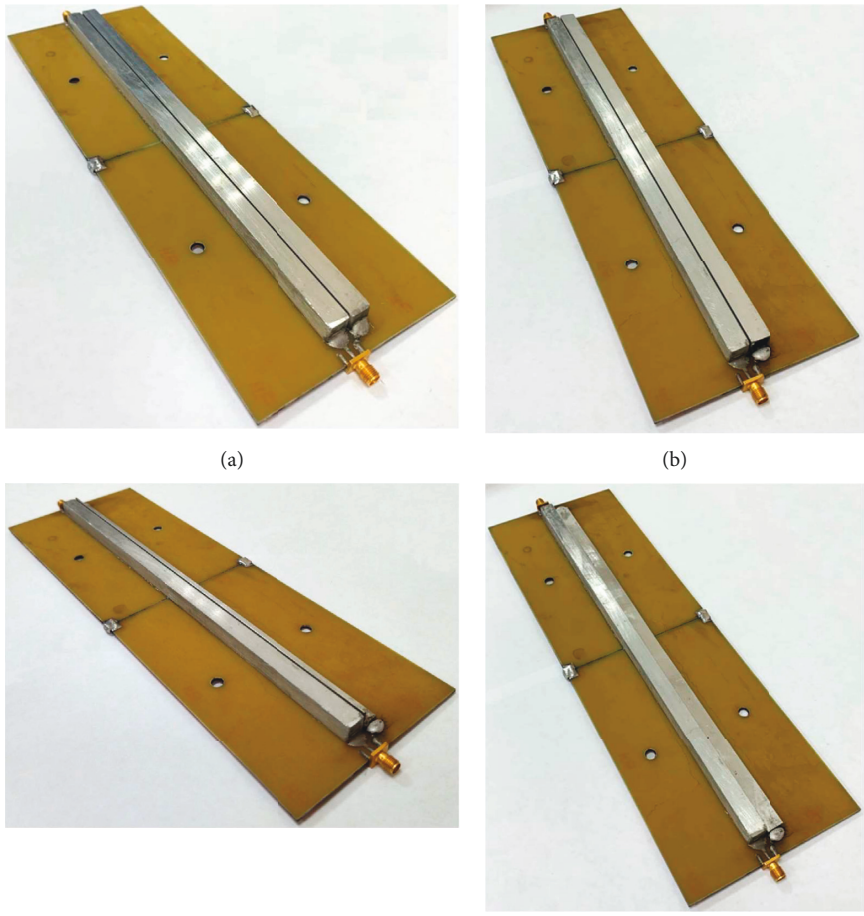

Figure 3: MF with a passive conductor: (a) solid, (b) hollow, (c) corner, and (d) thin.

the operation of redundant REE without failures. However, in regular situations, without failures, REE does not utilize the reserved units. Modal reservation (MR) is a type of cold redundancy that provides USP suppression by modal distortions [49]. Using MR to improve the reliability of vulnerable or critical units of UAVs also improves their interference immunity. There are many different structures with MR, which differ in application areas, the efficiency of USP suppression, and mass and size parameters [50, 51]. Of interest are reflection symmetric structures that provide the same USP suppression efficiency for each of the connected units [52]. They have good mass and size parameters, which allow their use in civil and military UAVs. Figure 7(a) shows a cross-section of the initial configuration of the proposed MR structure, which is a shielded four-layer printed circuit board. Figure 7(b) shows its connection diagram. In such a structure, internal conductors can connect power and ground circuits, while external conductors can be used for reserving particularly vulnerable or critical units of the UAV. The UAV enclosure can be used as a shielding surface. However, there may be apertures in the enclosure walls that reduce shielding effectiveness (SE). Shielding integrity can be provided by careful design, however, this task requires accurate solutions.

Figure 4: Vector network analyzer «Panorama» P4226 and an MF prototype with a corner passive conductor.

To reduce the resonance effects of the apertures, it is necessary to use TRIZ. By analyzing the existing methods of increasing SE, a technical solution was found. Thus, the space between the external conductors of the structure with a triple MR and the UAV enclosure can be filled with

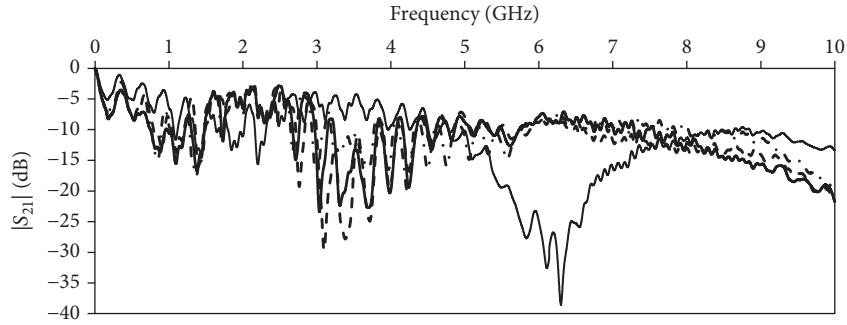

Figure 5: Measured frequency dependences $|S_{21}|$ of the MF with passive conductors: (–) solid, (- -) hollow, (- · -) corner, and (–) thin.

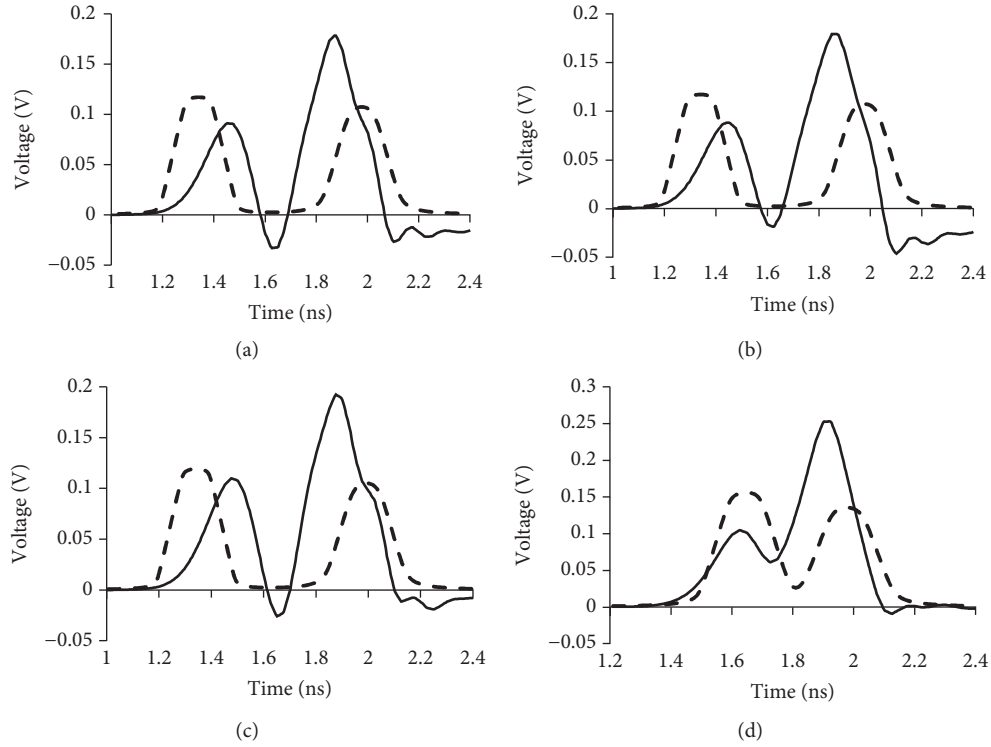

Figure 6: Voltage waveforms at the output of the MF with passive conductors: (a) solid, (b) hollow, (c) corner, and (d) thin, obtained by (- -) lossy simulation and (––) experimentally.

broadband radio-absorbing materials (RAM), for example, magnetodielectric ZIPSIL RPM-P1, which can effectively be used as a resonance absorber. The high values of ε_{r1} and μ_{r1} can improve the USP suppression by increasing the differences in the per-unit-length delays. The electrodynamic simulations of the modified configuration with a triple MR and RAM were performed to evaluate its time and frequency characteristics. The structure was simulated with the following geometric parameters from [53]: $s = 700\,\mu$m, $w = 1000\,\mu$m, $t = 35\,\mu$m, $H = 920\,\mu$m, $H_1 = 2000\,\mu$m, and $h = 510\,\mu$m. The dielectric and magnetodielectric electrical parameters were the following: $\varepsilon_r = 4.5$, $tg\delta = 0.025$, $\varepsilon_{r1} = 20$, $tg\delta_{\varepsilon_1} = 0.06$, $\mu_{r1} = 3$, and $tg\delta_{\mu_1} = 0.5$. To match the transmission line with the interference source U_s and the load, the resistances of all resistors (R) in the simulation were equal to 50 Ω. Frequency characteristics were analyzed in the range from 0 to 3 GHz. To analyze the time characteristics, two Gaussian pulses with a total duration of 0.8 and 2.4 ns were separately fed to the input of the reserved conductor (node V_1) (most of the energy is in the frequency range of 0 to 3 GHz and 0 to 1 GHz, respectively). To evaluate the effectiveness of suppressing such USPs, N-norms can be used [54]. They are also used to evaluate the possibility of dielectric electrical breakdown, and the burnout of connected elements. The analyzed norms and their characteristics from [55] are given in Table 2. The voltage waveforms of the decomposed pulses $U(t)$ are given as an argument in the equation.

Figure 8 shows the frequency dependences of $|S_{21}|$ and the voltage waveforms at the output of the reserved conductor (node V_2), which were obtained in the course of the electrodynamic simulation. The frequency characteristics

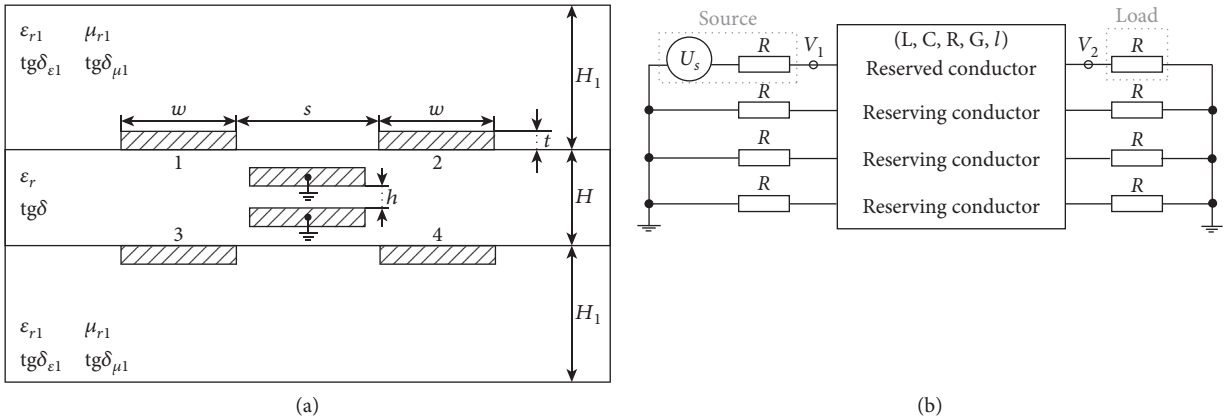

Figure 7: Reflection symmetric structure with triple MR: (a) cross-section and (b) connection diagram.

Table 2: N-norms description and application.

	N_1	N_2	N_3	N_4	N_5
Formula	$\lvert U(t)\rvert_{\max}$	$\lvert \mathrm{d}U(t)/\mathrm{d}t\rvert_{\max}$	$\lvert \int_0^t U(t)\mathrm{d}t\rvert_{\max}$	$\int_0^\infty \lvert U(t)\rvert \mathrm{d}t$	$\left\{\int_0^\infty \lvert U(t)\rvert^2 \mathrm{d}t\right\}^{1/2}$
Name	The peak value (absolute)	The peak derivative (absolute)	The peak pulse (absolute)	Rectified general pulse	The square root of the action integral
Application	Circuit failure/electric breakdown/electric arc effects	Component sparking/circuit failure	Dielectric breakdown (if U means the E field)	Equipment damage	Component burnout

show that both configurations have the characteristics of a low-pass filter. The use of RAM reduced the cutoff and first resonance frequencies of the structure with MR. The frequency response of the configuration with RAM decreases monotonically with increasing the frequency because of the presence of heavy losses in the magnetodielectric. The time response shows that modal distortions and losses significantly influence the USP waveform. Thus, both configurations decomposed the input pulse into a sequence of 4 pulses. Because of heavy dispersion, complete modal decomposition is not observed. However, both configurations attenuated USPs by several times.

Table 3 provides the values of the cutoff and first resonance frequencies, as well as the maximum voltage at the output of the structure under investigation. The calculated N-norms for the two USPs are given in Table 4.

Table 3 provides that the f_c value decreased by 150 MHz and reached 40 MHz. It is also seen that the f_r value decreased by 490 MHz. Changing these two parameters indicates an increase in the duration of the maximum possible interference pulse, which will be decomposed in the structure with MR. Table 4 provides that both structures significantly attenuated both USPs, and using RAM reduced the values of all norms. Thus, in the case of N_1, an additional attenuation of 1.87 times was obtained for USPs of 0.8 ns duration, and 2.51 times for USPs of 2.4 ns duration. Because of the strong dispersion, the N_2 value in the RAM configuration is much lower than that in the source configuration. At the same time, the maximum attenuation of the input excitation was 38 times for USPs with a duration of 0.8 ns. In the case of N_3 and N_4, there is also a decrease in the input excitation. Since there are no negative components in the waveform, the two norms will be identical. The use of RAM gives only a small advantage under these norms. In the case of N_5, large differences are observed. Thus, the use of RAM reduced the values of the last norm by at least a factor of 1.74 for both USPs.

7. Evaluation of USP Train Attenuation Possibility

The progress of USP generators is steadily continuing. Their impact on the onboard equipment of the UAVs is more effective than the impact of other types of electromagnetic pulses at the same values of electric field strengths. It is explained by the fact that the duration of interference and information signals commensurate, which leads to an increase in the probability of violating the information processed by the UAV control system [56]. Thus, because of the rapid development of digital computing technology, the increase in the volume and speed of data transmission, and the ability to remotely control UAVs in real time, there appears a need to ensure the stable operation of UAVs under the conditions of possible USP impact. However, modern devices have a number of disadvantages that do not allow full USP protection (insufficient processing speed, parasitic parameters, complexity, and high cost), which urges the development of new devices.

Known are USP protection devices working on the principle of modal filtration. The principle lies in using coupled transmission lines with inhomogeneous dielectric filling to decompose the input USP of a large amplitude into several pulses of smaller amplitudes. As mentioned earlier, one of the devices where modal filtration is implemented is a reflection symmetric modal filter (MF) [57]. However, this

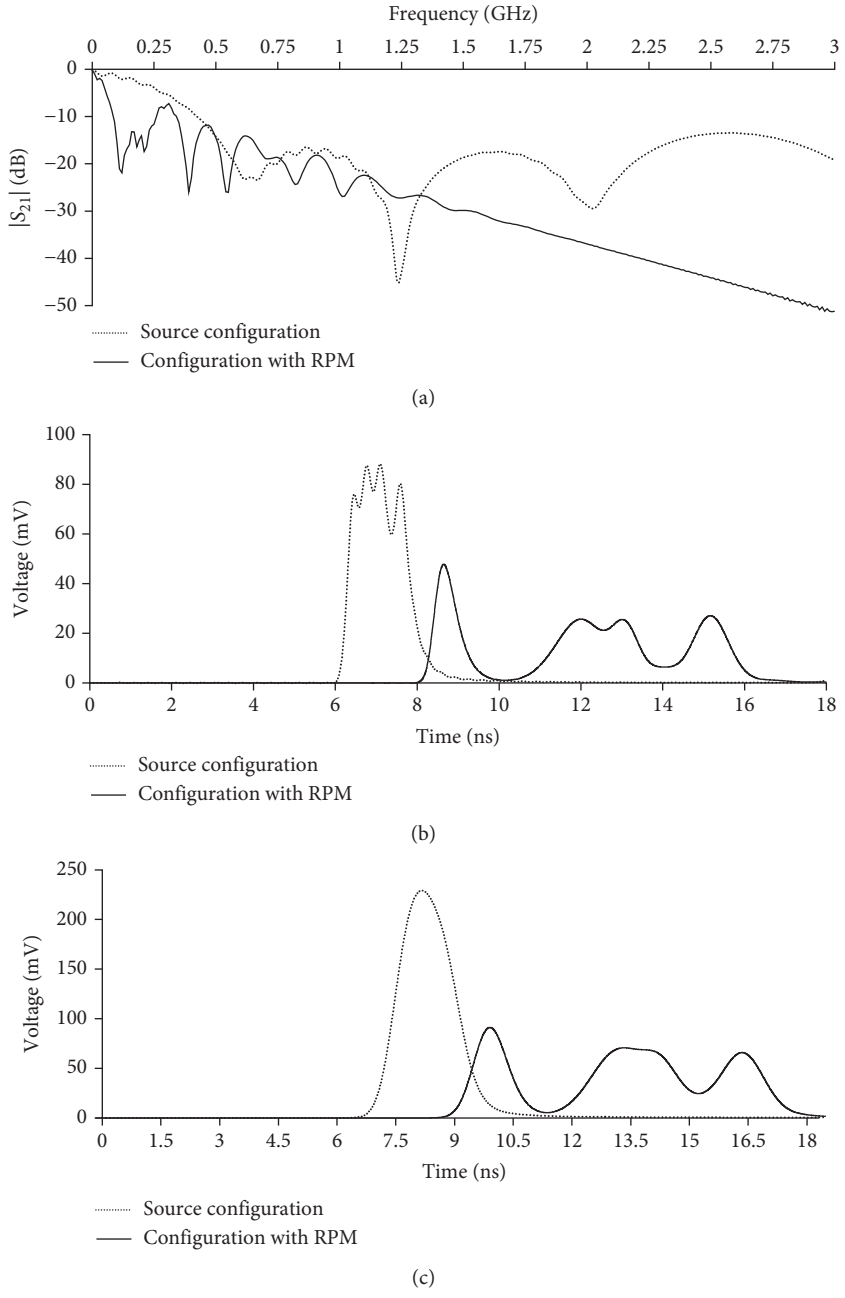

Figure 8: Characteristics of the two structures with MR: (a) frequency dependences of $|S_{21}|$, and output voltage waveforms for a USP with the duration of (b) 0.8 and (c) 2.4 ns.

Table 3: Cutoff and first resonance frequencies, as well as the maximum voltage at the output under the influence of USPs.

Parameters	f_c, MHz	f_r, MHz	U_{max}, V (0.8 ns)	U_{max}, V (2.4 ns)
Source configuration	190	610	0.088	0.229
Configuration with RAM	40	120	0.048	0.091

device has some disadvantages. An important parameter of the MF is the difference in modes' delays. The larger the difference, the longer the USP can be decomposed. Thus, the existing structure should be improved. In this case, it is effective to use TRIZ. By analyzing the existing methods of improving the MF, several solutions were found. One solution is to increase the value of the delay difference by increasing the length. However, it will result in an increase in the MF size and weight. Another solution is to increase the ε_r value, however, the cost of the device will increase. The use of TRIZ led to the idea that there is no need to change the cross-section of the reflection symmetric MF but only its boundary conditions. It was proposed to obtain a reflection symmetric meander line (ML) from a reflection symmetric MF by

Table 4: N-norms for USPs of different durations.

Durations of the USP	Type of configuration	N_1	N_2	N_3	N_4	N_5
0.8 ns	Input excitation	1	$5.32 \cdot 10^9$	$285 \cdot 10^{-12}$	$285 \cdot 10^{-12}$	$14.2 \cdot 10^{-6}$
	Source configuration	0.088	$0.32 \cdot 10^9$	$136 \cdot 10^{-12}$	$136 \cdot 10^{-12}$	$2.95 \cdot 10^{-6}$
	Configuration with RAM	0.047	$0.14 \cdot 10^9$	$126 \cdot 10^{-12}$	$126 \cdot 10^{-12}$	$1.69 \cdot 10^{-6}$
2.4 ns	Input excitation	1	$1.77 \cdot 10^9$	$856 \cdot 10^{-12}$	$856 \cdot 10^{-12}$	$24.6 \cdot 10^{-6}$
	Source configuration	0.229	$0.28 \cdot 10^9$	$396 \cdot 10^{-12}$	$396 \cdot 10^{-12}$	$8.09 \cdot 10^{-6}$
	Configuration with RAM	0.091	$1.37 \cdot 10^9$	$375 \cdot 10^{-12}$	$375 \cdot 10^{-12}$	$4.56 \cdot 10^{-6}$

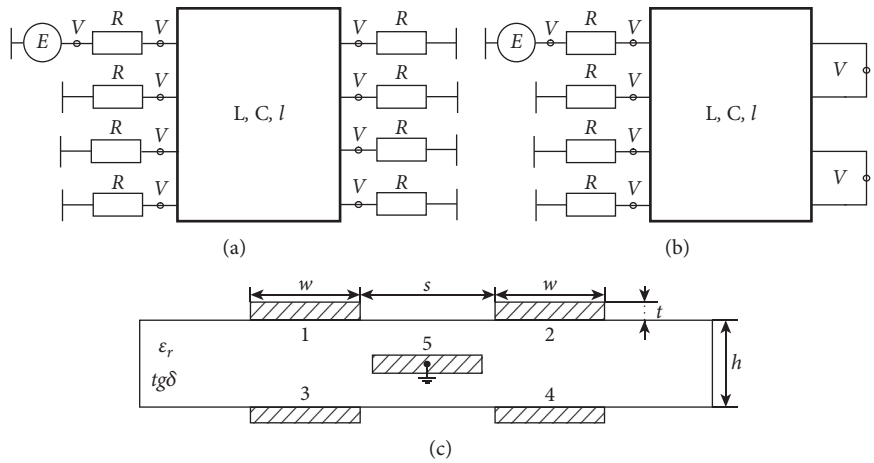

Figure 9: Equivalent circuits of reflection symmetric (a) MF, (b) ML, and their (c) cross-section.

electrically connecting the conductors at the ends of the line with bridges, instead of resistive ends to ground. In this case, the length and dimensions will remain unchanged, and the delay difference will increase by 2 times.

The main parameters of a USP are voltage amplitude, pulse duration, and steepness of its front, type, and width of the spectrum, as well as the number of consecutive pulses and the time intervals between them. In a real situation, USPs are generated in the form of a train with a certain frequency or repetition period. In this case, the effectiveness of the impact increases with an increase of its repetition frequency. In this regard, the analysis of the modal decomposition of USP train in reflection symmetric MFs and MLs is relevant.

The simulations were performed in the ADS 2020 software. The time characteristics were obtained using the inverse Fourier transform with the approach from [48]. Initially, S-parameters of the structures were measured with a vector network analyzer «Panorama» P4226 in the frequency range from 10 MHz to 20 GHz. Then, a two-port device was set in the ADS software, which was defined by the frequency characteristics obtained during the measurements. After that, the influence in the form of a train of USPs was applied to its input. Equivalent circuits of a reflection symmetric MF and an ML are shown in Figures 9(a) and 9(b), respectively. The cross-section is shown in Figure 9(c), where w and t are the width and thickness of the conductors (1075 and 35 μm), s is the distance between the conductors (700 μm), h is the dielectric thickness (1000 μm), and ε_r is the relative permittivity (4.5). The signal of 4 pulses with repetition periods (T) equal to 0.5, 1, and 2 ns was selected as an excitation. The amplitude of each pulse is 1 V, the duration of the front, fall, and flat top are 50 ps each, and the total duration (t_Σ) is 150 ps.

Figure 10 shows the simulation results for the reflection symmetric MFs and MLs excited by a USP train, and Table 5 provides the amplitudes ($U_{\max}$) at the output of the structures.

It follows from Figure 10 that the superposition of the decomposition pulse sequences of individual USPs from the train increases the voltage amplitudes at the MF and ML outputs as the T value decreases. At $T = 2$ ns, there is a division of each pulse from the USP train into a separate sequence of decomposition pulses. Therefore, with the fixed values of T and the duration of each pulse from the train, their complete decomposition is possible if the value of T is greater than or equal to the total duration of the sequence of decomposition pulses of one USP.

8. Using an ML as a USP Protection Means

Consider an ML to attenuate a USP amplitude. It is known that in one turn of an ML in air dielectric filling (or an air ML), the USP can be decomposed into 2 pulses (crosstalk and main signal) of smaller amplitudes [43], and in a turn of a microstrip ML, it is decomposed into 3 pulses (crosstalk and pulses of odd and even modes) of even smaller amplitudes [58]. Hence, for instance, the USP attenuation in the air ML was 1.6 times, and in the microstrip, it was 2.4 times. Moreover, the researchers managed to decompose a USP into as many as 4 pulses of smaller amplitudes [59]. The

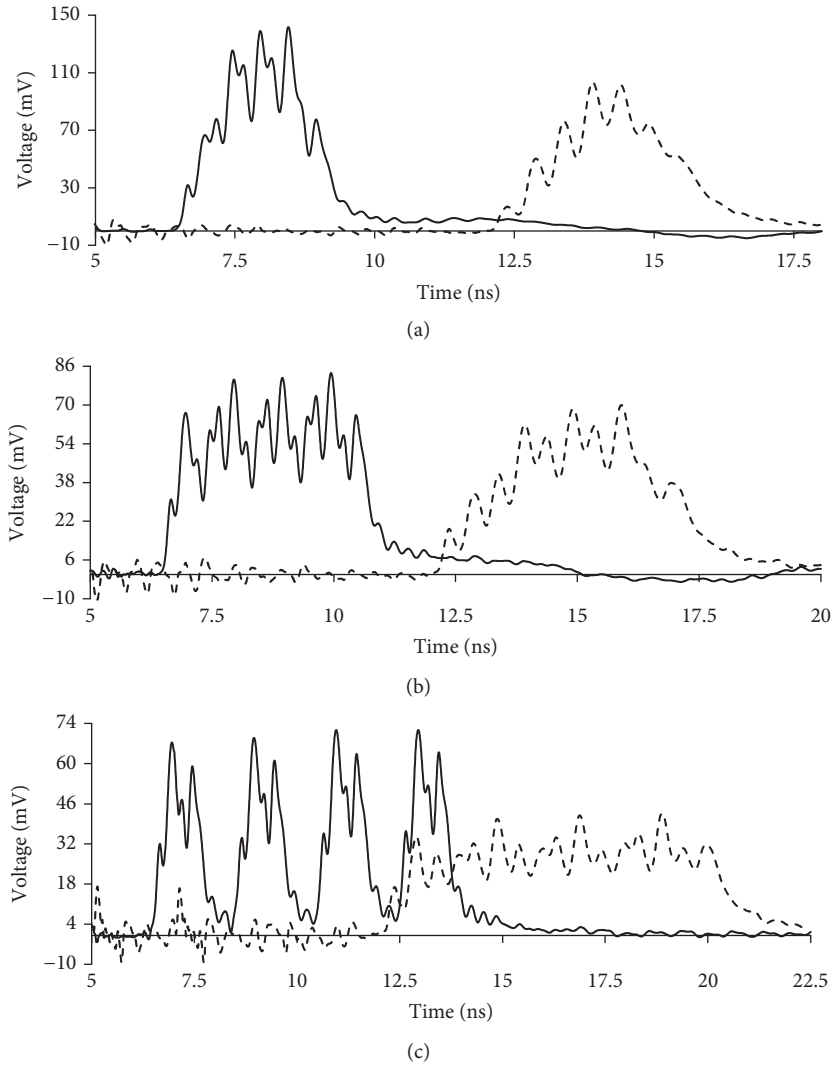

Figure 10: Voltage waveforms at the output of the reflection symmetric (–) MF and (- -) ML when excited by a USP train with repetition periods of (a) 0.5, (b) 1, and (c) 2 ns.

Table 5: Amplitudes at the output of the structures.

Repetition period of pulses in the USP train (ns)	0.5	1	2
U_{max} at the output of the reflection symmetric MF (mV)	141.39	82.27	69.45
U_{max} at the output of the reflection symmetric ML (mV)	100.97	69.71	41.71

research on the ML application to protect against USPs proved the possibility to increase the USP attenuation in the line. Thus, because of the asymmetry in the cross-section of a microstrip ML and the addition of another passive conductor [60], the USP attenuation in the line was as much as 5.4 times. Another resource is ML cascading [61], which allowed for the 5-time USP attenuation in the MSL with 2 turns connected in the cascade. When the line had 3 turns, the attenuation was 8 times: 4 turns–20 times, and 5 turns–33 times. Finally, the ML and MF can form a hybrid device based on their cascade connection. Thus, the cascade connection of a 3-conductor MF and a turn of a meander MSL allowed for the 10-time USP attenuation [62]. The structures based on a cascade connection of 3 and 4-conductor MF and the ML with a broadside coupling enabled as much as 12-time attenuation of the USP [63]. Note that these publications formulated conditions that allow complete USP decomposition for its maximum attenuation. These conditions are directly related to the matrices of the secondary parameters of the structures, which, in turn, are determined by their geometric parameters. These results were revealed with the help of TRIZ and previously developed approaches and methods.

9. Discussion

For the first time, the authors propose a set of diverse approaches and methods to solve the problem of providing the EMC of EMI-based functional destruction means with other REE as part of the UAV countermeasures complex. The

feasibility of the proposed approach has been demonstrated using some examples.

(1) Modal filtration

Modal filtration technology underlies a number of approaches aimed to solve the problem of ensuring EMC for both UAV countermeasure systems and «friendly» UAVs. At the same time, the very essence of the decomposition of conductive pulse excitations of short duration into a sequence of pulses with smaller amplitudes is valid for a wide range of MFs. However, an important factor is the possibility of using the available interconnects of a specific REE instead of a separate printed circuit board. For instance, such options that can be employed are as follows: the enclosure as a ground return plane, the free space on the printed circuit board, the existing cables and cable assemblies (replacement or modernization) as part of the REE, and the conventional printed conductors (with proper routing).

(2) Method of hollow and thin passive conductors

The measurement results confirm that the exciting pulse can be decomposed at the end of the active conductor of the MF when a solid passive conductor is replaced with a hollow, corner, or thin conductor. The consistency of the output voltage waveforms obtained experimentally and during the simulation was achieved. It was shown that the measured MFs had a bandwidth of about 77–82 MHz, and the values of the maximum output voltage were 5.6, 5.61, 5.2, and 4 times less than the EMF amplitude for the MFs with solid, hollow, corner, and thin passive conductors, respectively. Finally, it was estimated that when a solid passive conductor was replaced with a hollow one, it was possible to achieve a gain in mass by 3 times, with a corner conductor by 5.5 times, and with a thin conductor by 10 times. In this case, the decomposition of the USP into a sequence of pulses of smaller amplitudes is preserved.

(3) Magnetodielectric in structures with modal reservation

The application of TRIZ approach made it possible to design a device with a triple MR, which has improved interference protection characteristics. Using magnetodielectrics, it became possible to shift the resonant frequencies of the enclosure and suppress emissions. The N-norms of decomposed pulses were evaluated using two different durations of USPs and revealed the high efficiency of the investigated structure with MR in suppressing dangerous conducted interference.

(4) The evaluation of USP train attenuation possibility

In the considered example, the reflection symmetric MF attenuated the USP by 3, 6, and 7 times, and the ML by 5, 7, and 12 times at repetition periods of 0.5, 1, and 2 ns, respectively. More effective attenuation in the ML is explained by the fact that the time intervals between the decomposition pulses of one USP is 2 times longer than that in the MF. The construction of such a device, which retains the dimensions of the original one and at the same time has improved characteristics, was possible, thanks to the use of the TRIZ approach in the development process.

(5) Using an ML as a USP protection means

A further increase in the attenuation of a USP in an ML (relative to the data in the main part of the study) and the applicability of MLs in UAVs will be carried out using verified approaches and methods, as well as, if necessary, new ones using the TRIZ approach. Now, it seems attractive to take advantage of an increase in the number of passive conductors, the use of asymmetry, cascading, as well as the hybridization of new structures based on MLs and MFs to increase USP attenuation. The approaches and methods discussed will allow for the synthesis of these devices while considering the requirements for the UAVs in which they will be used.

Thus, a careful study of the presented approaches and techniques resulted in a unified blended methodology that could further motivate the formulation of unique private methods. Their results will be represented by specific technical solutions aimed to ensure the EMC of specific UAV countermeasures systems, as well as «friendly» UAVs during potential military operations. As a result, there is a prospect of eliminating «enemy» UAVs (by means of EMI-based functional destruction means), without damaging «friendly» infrastructure and UAVs. On top of all, it can be done cost-effectively.

10. Conclusions

The study demonstrates the expediency of using a number of proposed approaches and methods exemplified by specific structures and under specific interference effects. A unique methodology was proposed for ensuring the EMC of UAV countermeasure systems that incorporate EMI-based functional destruction means. The obtained results are highly relevant and their use is incredibly broad because they imply additional protection (within the proposed methodology). It is true for REE operating as part of the UAV countermeasures complex and for «friendly» UAVs.

The next step is to create the valid design of the methodology, taking into account the proposed methods and approaches. For this purpose, it is important to make an extensive review and analysis of well-known methods for ensuring the EMC of critical components and systems. In addition, it is important to systematize the well-known means of EMI-based functional destruction means, as well as UAVs.

Data Availability

The data used to support this study are available from the corresponding author upon request.

Conflicts of Interest

The authors declare that there are no conflicts of interest.

Acknowledgments

The reported study was funded by the Russian Science Foundation (22-29-01331).

References

[1] V. N. Zhuravlev and P. V. Zhuravlev, "Usage of unmanned aerial vehicles in general aviation: current situation and prospects," *Civil Aviation High Technologies (Nauchnyi Vestnik MGTU GA)*, vol. 4, pp. 156–164, 2016, in Russian.

[2] S. A. Lyasheva, M. V. Medvedev, and M. P. Shleimovich, "Terrain object recognition in unmanned aerial vehicle control system," izvestiya vysshikh uchebnykh zavedenii," *Aviatsionnaya Tekhnika*, vol. 3, pp. 64–66, 2014, in Russian.

[3] S. A. Lyasheva, M. V. Medvedev, and M. P. Shleymovich, "Image wavelet compression in unmanaged vehicle control systems," *Vestnik Kazanskogo gosudarstvennogo tekhnicheskogo universiteta im. A.N. Tupoleva*, vol. 4, pp. 218–222, 2013, in Russian.

[4] M. Nuriev, "Physical simulation of an unmanned aerial vehicle electronic means noise immunity," *Trudy MAI*, vol. 102, no. 1–15, 2018, in Russian.

[5] Z. M. Gizatullin, R. M. Gizatullin, and M. G. Nuriev, "Mathematical models for physical modeling problems of electromagnetic compatibility," *Power Engineering: Research, Equipment, Technology*, vol. 1–2, pp. 115–122, 2015, in Russian.

[6] M. A. Holland, "Counter–drone systems," center for the study of the drone at bard college," *Feburary*, vol. 20, p. 23, 2018.

[7] C. rogue drones, *FICCI Committee on Drones*, p. 31, FICCI, New Delhi, India, 2018.

[8] E. de Visser, M. S. Cohen, and M. LeGoullon, "A design methodology for controlling, monitoring, and allocating unmanned vehicles," in *Proceedings of the Third International Conference on Human Centered Processes (HCP–2008)*, pp. 1–5, Delft, The Netherlands, June 2008.

[9] B. H. Sheu, C. C. Chiu, W. T. Lu, C. I. Huang, and W. P. Chen, "Development of UAV tracing and coordinate detection method using a dual–Axis rotary platform for an anti–UAV system," *Applied Sciences*, vol. 9, no. 13, pp. 1–17, 2019.

[10] M. Kratky and V. Minarik, "The non-destructive methods of fight against UAVs," in *Proceedings of the 2017 International Conference on Military Technologies (ICMT)*, pp. 690–694, Brno, Czech Republic, June 2017.

[11] K. Y. Sakharov, A. V. Sukhov, V. L. Ugolev, and Y. M. Gurevich, "Study of UWB electromagnetic pulse impact on commercial unmanned aerial vehicle," in *Proceedings of the 2018 International Symposium on Electromagnetic Compatibility (EMC EUROPE)*, pp. 40–43, Amsterdam, Netherlands, August 2018.

[12] Y. Chen, D. Zhang, E. Cheng, and X. Wang, "Investigation on susceptibility of UAV to radiated IEMI," in *Proceedings of the 2018 IEEE International Symposium on Electromagnetic Compatibility and 2018 IEEE Asia–Pacific Symposium on Electromagnetic Compatibility (EMC/APEMC)*, pp. 718–722, Suntec City, Singapore, May 2018.

[13] C. Gao, Z. Xue, W. Li, and W. Ren, "The influence of electromagnetic interference of HPM on UAV," in *Proceedings of the 2021 International Conference on Microwave and Millimeter Wave Technology (ICMMT)*, pp. 1–3, Nanjing, China, May 2021.

[14] D. Zhang, E. Cheng, H. Wan, X. Zhou, and Y. Chen, "Prediction of electromagnetic compatibility for dynamic datalink of UAV," *IEEE Transactions on Electromagnetic Compatibility*, vol. 61, no. 5, pp. 1474–1482, 2019.

[15] X. Gao, H. Jia, Z. Chen, G. Yuan, and S. Yang, "UAV security situation awareness method based on semantic analysis," in *Proceedings of the 2020 IEEE International Conference on Power, Intelligent Computing and Systems (ICPICS)*, pp. 272–276, Shenyang, China, July 2020.

[16] J. L. Esteves, E. Cottais, and C. Kasmi, "Unlocking the access to the effects induced by IEMI on a civilian UAV," in *Proceedings of the 2018 International Symposium on Electromagnetic Compatibility (EMC EUROPE)*, pp. 48–52, Amsterdam, Netherlands, August 2018.

[17] M. Adamski, "Analysis of propulsion systems of unmanned aerial vehicles," *Journal of Marine Engineering & Technology*, vol. 16, no. 4, pp. 291–297, 2017.

[18] A. Haider, "A comprehensive approach to countering unmanned aircraft systems," *Joint Air Power Competence Centre*, pp. 1–6, 2020, https://www.japcc.org/books/a-comprehensive-approach-to-countering-unmanned-aircraft-systems/.

[19] Y. Li, Q. Ding, K. Li, S. Valtchev, S. Li, and L. Yin, "A survey of electromagnetic influence on UAVs from an EHV power converter stations and possible countermeasures," *Electronics*, vol. 10, no. 6, p. 701, 2021.

[20] P. Wang, C. Wu, Y. Wang, F. Xu, and J. Chen, "Statistics and analysis of foreign military medium and heavy UAV accidents," in *Proceedings of the SPIE 11562, AOPC 2020: Advanced Laser Technology and Application*, Beijing, China, November 2020.

[21] S.-G. Kim, E. Lee, I.-P. Hong, and J.-G. Yook, "Review of intentional electromagnetic interference on UAV sensor modules and experimental study," *Sensors*, vol. 22, no. 6, p. 2384, 2022.

[22] P. Szczupak and T. Kossowski, "Response of drone electronic systems to a standardized lightning pulse," *Energies*, vol. 14, no. 20, p. 6547, 2021.

[23] I. V. Suzdaltsev, S. F. Chermoshencev, and N. Y. Bogula, "Genetic algorithm for onboard equipment placement inside the unmanned aerial vehicle fuselage," in *Proceedings of the 2016 XIX IEEE International Conference on Soft Computing and Measurements (SCM)*, pp. 262–264, St. Petersburg, Russia, May 2016.

[24] I. Bennageh, H. Mahmoudi, and M. Labbadi, "Impact of the electromagnetic environment on UAV's datalink," *IOP Conference Series: Earth and Environmental Science*, vol. 785, pp. 1–6, 2021.

[25] S. G. Garcia, "UAVEMI project: numerical and experimental EM immunity assessment of UAV for HIRF and lightning indirect effects," in *Proceedings of the 2016 ESA Workshop on Aerospace EMC (Aerospace EMC)*, pp. 1–5, Valencia, Spain, May 2016.

[26] Y. Wu, Q. Ma, and P. Xu, "Progress of electromagnetic compatibility design for unmanned aerial vehicles," *MATEC Web of Conferences*, vol. 316, no. 11, Article ID 4008, 2020.

[27] G. Lubkowski, M. Lanzrath, L. C. Lavau, and M. Suhrke, "Response of the UAV sensor system to HPEM attacks," in *Proceedings of the 2020 International Symposium on Electromagnetic Compatibility*, pp. 1–6, Rome, Italy, September 2020.

[28] J. Junmin, S. Qijun, and G. Yougang, "The simulation of interference between the unmanned aerial vehicle (UAV)

system and the CDMA system based on Simulink," in *Proceedings of the The 2006 4th Asia–Pacific Conference on Environmental Electromagnetics*, pp. 750–754, Dalian, China, August 2006.

[29] R. Geise, A. Weiss, T. Fritzel, R. Strauß, F. T. Faul, and T. F. Eibert, "Interference measurements of a high power cable–bound unmanned aerial vehicle," in *Proceedings of the 2019 13th European Conference on Antennas and Propagation (EuCAP)*, pp. 1–5, Krakow, Poland, April 2019.

[30] S. Lin, M. Cho, M. Lin, W. Hu, and J. Sun, "EMC considerations in transponder antenna design for tactical automatic landing systems," in *Proceedings of the TENCON 2019 – 2019 IEEE Region 10 Conference (TENCON)*, pp. 235–237, Kochi, India, October 2019.

[31] M. Pous, S. Fernández, M. Añón, M. R. Cabello, L. D. Angulo, and F. Silva, "Time domain double–loaded electromagnetic field probe applied to unmanned air vehicles," in *Proceedings of the 2018 IEEE Symposium on Electromagnetic Compatibility, Signal Integrity and Power Integrity (EMC, SI & PI)*, pp. 30–35, Long Beach, CA, USA, August 2018.

[32] R. J. Perez, "EMC considerations for unmanned aerial vehicles," in *Handbook of Aerospace Electromagnetic Compatibility*, pp. 603–619, IEEE, 2019.

[33] D. Zhang, X. Zhou, E. Cheng, H. Wan, and Y. Chen, "Investigation on effects of HPM pulse on UAV's datalink," *IEEE Transactions on Electromagnetic Compatibility*, vol. 62, no. 3, pp. 829–839, June 2020.

[34] S. I. Makarenko, "Protivodejstvie Bespilotnym Letatel'nym apparatam. Monografiya," *Naukoemkie tekhnologii*, vol. 204, 2020 in Russian.

[35] N. Mora, F. Vega, G. Lugrin, R. Farhad, and R. Marcos, "Study and classification of potential IEMI sources," System and assessment notes," *Note*, vol. 41, p. 92, 2014.

[36] T. R. Gazizov, "Design of electronic systems protected from electromagnetic terrorism," in *Proceedings of the 15–th Int. Wroclaw Symp. on EMC*, pp. 469–472, Poland, Wroclaw, June 2000.

[37] A. T. Gazizov, A. M. Zabolotsky, and T. Rashitovich Gazizov, "UWB pulse decomposition in simple printed structures," *IEEE Transactions on Electromagnetic Compatibility*, vol. 58, no. 4, p. 1136, 2016.

[38] A. O. Belousov and T. R. Gazizov, "Method for tracing modal filter conductors," 2750393, 2021.

[39] T. R. Gazizov, P. E. Orlov, A. M. Zabolotsky, and S. P. Kuksenko, "New concept of critical infrastructure strengthening," in *Proceedings of the 13th Int. Conf. of Numerical Analysis and Applied Mathematics*, pp. 1–3, Rhodes, Greece, September 2015.

[40] A. O. Belousov, A. V. Medvedev, E. B. Chernikova, T. R. Gazizov, and Z. Alexander, "Switching order after failures in symmetric protective electrical circuits with triple modal reservation," *Symmetry*, vol. 13, no. 6, pp. 1–22, Article ID 1074, 2021.

[41] A. M. Zabolotsky, T. R. Gazizov, A. G. Bova, and W. A. Radasky, "Dangerous pulse excitation of coupled lines," in *Proceedings of the 2006 17th International Zurich Symposium on Electromagnetic Compatibility*, pp. 164–167, Singapore, March 2006.

[42] M. E. Komnatnov, T. R. Gazizov, I. I. Nikolaev, and A. A. Demakov, "Drozdova Method for manufacturing power transmission line with spiral cross–section and device based on its basis," 2749558, 2021.

[43] R. Surovtsev, T. Gazizov, and A. Zabolotsky, "Pulse decomposition in the turn of meander line as a new concept of protection against UWB pulses," in *Proceedings of the 2015 International Siberian Conference on Control and Communications (SIBCON)*, pp. 1–5, Omsk, Russia, May 2015.

[44] A. A. Ivanov, M. E. Komnatnov, and M. E. Komnatnov, "Semi-analytical method for evaluating shielding effectiveness of an enclosure with an aperture," *Proceedings of Tomsk State University of Control Systems and Radioelectronics*, vol. 24, no. 1, pp. 16–23, 2021.

[45] A. A. Ivanov, A. V. Demakov, and M. E. Komnatnov, "Semi–analytical approach for calculating shielding effectiveness of an enclosure with a filled aperture," *Electrica*, vol. 22, no. 2, pp. 220–225, 2022.

[46] S. P. Kuksenko, "Preliminary results of TUSUR University project for design of spacecraft power distribution network: EMC simulation," *IOP Conference Series: Materials Science and Engineering*, vol. 560, pp. 1–7, Article ID 12110, 2019.

[47] A. O. Belousov, E. B. Chernikova, and M. A. Samoylichenko, "From symmetry to asymmetry: the use of additional pulses to improve protection against ultrashort pulses based on modal filtration," *Symmetry*, vol. 12, no. 7, pp. 1–38, 2020.

[48] R. Vauché, "Experimental time–domain study for bandpass negative group delay analysis with lill–shape microstrip circuit," *IEEE Access*, vol. 9, pp. 24155–24167, Article ID 24155, 2021.

[49] T. R. Gazizov, P. E. Orlov, A. M. Zabolotsky, and S. P. Kuksenko, "New Concept of Critical Infrastructure Strengthening," *AIP Conference Proceedings*, vol. 1738, Article ID 440007, Rhodes, Greece, 2016.

[50] Y. S. Zhechev, A. V. Zhecheva, A. A. Kvasnikov, and A. M. Zabolotsky, "Using N-norms for analyzing symmetric protective electrical circuits with triple modal reservation," *Symmetry*, vol. 13, no. 12, p. 2390, 2021.

[51] P. E. Orlov, A. V. Medvedev, and V. R. Sharafutdinov, "Quasistatic simulation of ultrashort pulse propagation in the spacecraft autonomous navigation system power circuit with modal reservation," in *Proceedings of the 2018 19th International Conference of Young Specialists on Micro/Nanotechnologies and Electron Devices (EDM)*, pp. 1–6, Erlagol, Russia, July 2018.

[52] Y. S. Zhechev, E. B. Chernikova, and A. O. Belousov, "Research of the new structure of reflection symmetric modal filter," in *Proceedings of the 2019 20th International Conference of Young Specialists on Micro/Nanotechnologies and Electron Devices (EDM)*, pp. 108–112, Erlagol, Altai Republic, July 2019.

[53] Y. S. Zhechev, "Experimental study of the buried vias effect on reflection symmetric modal filter performance," in *Proceedings of the 2020 21st International Conference of Young Specialists on Micro/Nanotechnologies and Electron Devices (EDM)*, pp. 200–204, Chemal, Russia, July 2020.

[54] C. E. Baum, *Mathematics Notes. Note*, p. 63, 1979.

[55] D. V. Giri, ""High–Powered Electromagnetic Radiators: Nonlethal Weapons and Other Applications," *Electromagnetics library*, Harvard University Press, Cambridge, MA, 2004.

[56] Y. V. Yukhanov, T. Y. Privalova, A. Y. Yukhanov, V. I. Andrianov, A. G. Ostrovsky, and V. F. Los, "Peculiarities of videopulse scanning antenna array design," in *Proceedings of the 2006 3rd International Conference on Ultrawideband and Ultrashort Impulse Signals*, pp. 85–89, Sevastopol, Ukraine, September 2006.

[57] E. B. Chernikova and A. A. Ivanov, "Using composite insulating materials to improve modal filter performance," in *Proceedings of the 2020 21st International Conference of Young*

Specialists on Micro/Nanotechnologies and Electron Devices (EDM), pp. 187–190, Chemal, Russia, July 2020.

[58] R. S. Surovtsev, A. V. Nosov, and A. M. Zabolotsky, "Simple method of protection against UWB pulses based on a turn of meander microstrip line," in *Proceedings of the 2015 16th International Conference of Young Specialists on Micro/Nanotechnologies and Electron Devices*, pp. 175–177, Erlagol, Russia, July 2015.

[59] A. V. Nosov and R. S. Surovtsev, "Revealing new possibilities of ultrashort pulse decomposition in a turn of asymmetrical meander delay line," in *Proceedings of the 2020 21st International Conference of Young Specialists on Micro/Nanotechnologies and Electron Devices (EDM)*, pp. 149–153, Chemal, Russia, July 2020.

[60] A. V. Nosov and R. S. Surovtsev, "Ultrashort pulse decomposition in the turn of a meander microstrip line with a passive conductor," *Journal of Physics: Conference Series*, vol. 1862, pp. 1–6, 2021.

[61] G. Y. Kim, A. V. Nosov, and R. S. Surovtsev, "Conditions for ultrashort pulse decomposition in multi–cascade protection devices based on meander microstrip lines," *Journal of Physics: Conference Series*, vol. 1679, pp. 1–6, 2020.

[62] A. V. Nosov, A. O. Belousov, and R. S. Surovtsev, "Simulating hybrid protection against ultrashort pulse based on its modal decomposition," *Journal of Physics: Conference Series*, vol. 1353, pp. 1–6, 2019.

[63] G. Kim, A. Nosov, and R. Surovtsev, "Ultrashort pulse decomposition in hybrid protection devices based on the cascade–connected modal filter and meander line with broad–side coupling," in *Proceedings of the 2021 IEEE 22nd International Conference of Young Professionals in Electron Devices and Materials (EDM)*, pp. 163–166, Souzga, the Altai Republic, Russia, July 2021.